Enhancement of hepatic differentiation from induced pluripotent stem cells by suppressing epithelial–mesenchymal transition

VISUAL ABSTRACT

Enhancement of hepatic differentiation from induced pluripotent stem cells by suppressing epithelial–mesenchymal transition

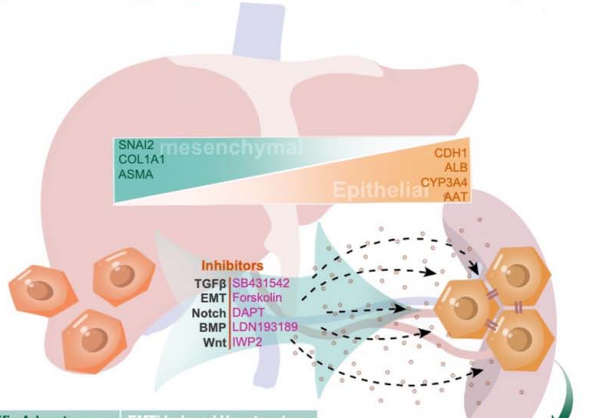

Specific Advantages	EMTI Induced Hepatocytes
Differentiation Efficiency	Capable of maintaining for over 60 days
Functional Maturity	High functional maturity, closer to adult hepatocytes
Cell Morphology	Maintains hepatocyte-like morphology, reduces variability
Hepatic Functional Markers	High expression levels, strong stability
Long-Term Culture	Achieves long-term culture with good functional retention
In Vivo Engraftment Efficiency	Improved survival rate post-transplant, approximately 4%

Received: 13 July 2024 | Accepted: 7 December 2024

DOI: 10.1097/HC9.0000000000000702

ORIGINAL ARTICLE

OPEN

Enhancement of hepatic differentiation from induced pluripotent stem cells by suppressing epithelial–mesenchymal transition

Na Li[1,2,3] | Rui Wei[4] | Yangyang Yuan[5,6] | Mingdan Deng[5,6] | Yang Hu[1,2] | Chi-Wa Cheng[1,2] | Jiayin Yang[7,8] | Wai-In Ho[1,2] | Ka-Wing Au[1,2] | Yiu-Lam Tse[1,2] | Fei Li[1,2] | Xinyi Wu[1,2] | Yee-Man Lau[1,2] | Songyan Liao[1,2,5] | Stephanie Ma[5,6] | Pentao Liu[5,6] | Kwong-Man Ng[1,2,5] | Miguel A. Esteban[2,3,8,9,10] | Hung-Fat Tse[1,2,3,5,8,11,12]

[1]Department of Medicine, The Cardiology Division, Li Ka Shing Faculty of Medicine, The University of Hong Kong, Hong Kong SAR, China

[2]Hong Kong-Guangdong Stem Cell and Regenerative Medicine Research Centre, The University of Hong Kong and Guangzhou Institutes of Biomedicine and Health, Hong Kong SAR, China

[3]Cardiac and Vascular Center, The University of Hong Kong-Shenzhen Hospital, Shenzhen, China

[4]Department of Gastroenterology and Hepatology, Guangdong Provincial People's Hospital (Guangdong Academy of Medical Sciences), Southern Medical University, Guangzhou, China

[5]Centre for Stem Cell Translational Biology, The University of Hong Kong, Hong Kong SAR, China

[6]School of Biomedical Sciences, Li Ka Shing Faculty of Medicine, The University of Hong Kong, Hong Kong SAR, China

[7]Cell Inspire Therapeutics Co., Ltd and Cell Inspire Biotechnology Co., Ltd, Shenzhen, China

[8]Laboratory of Integrative Biology, Guangzhou Institutes of Biomedicine and Health, Chinese Academy of Sciences, Guangzhou, China

[9]Joint School of Life Sciences, Guangzhou Medical University and Guangzhou Institutes of Biomedicine and Health, Guangzhou, China

[10]3DC STAR, Spatiotemporal Campus at BGI Shenzhen, Shenzhen, China

[11]Advanced Biomedical Instrumentation Centre, Hong Kong Science Park, New Territories, Hong Kong

[12]Centre for Regenerative Medicine and Health, Hong Kong Institute of Science & Innovation, Chinese Academy of Sciences, Hong Kong SAR, China

Correspondence
Hung-Fat Tse, Department of Medicine, Cardiology Division, School of Clinical Medicine, The University of Hong Kong, Queen Mary Hospital, Hong Kong, China.
Email: hftse@hku.hk

Abstract

Background: Induced pluripotent stem cells induced hepatocytes (iHeps) are widely used in modeling human liver diseases and as a potential cell source for replacement therapy. However, most iHeps are relatively immature and challenging to maintain for long-term in vitro culture.

Methods: We optimized the differentiation protocol by addition of a combination of small molecules to inhibit epithelial–mesenchymal transition (EMT)

Abbreviations: ACTA2, actin alpha 2, smooth muscle; COL1A1, collagen type I alpha 1 chain; E-cadherin, epithelial cadherin; EMT, epithelial–mesenchymal transition; EMTi, EMT inhibitor; FAH, fumarylacetoacetate hydrolase; FRG mice, Fah$^{-/-}$/Rag2$^{-/-}$/Il2rg$^{-/-}$ mice; hALB, human albumin; iHeps, iPSC-derived hepatocytes; iPSCs, induced pluripotent stem cells; PAS, periodic acid-Schiff; PHHs, primary human hepatocytes; SNAI2, snail family transcriptional repressor 2; TGFβ, transforming growth factor beta

Na Li, Rui Wei, and Yangyang Yuan have contributed equally to this work and are co-first authors.

Supplemental Digital Content is available for this article. Direct URL citations are provided in the HTML and PDF versions of this article on the journal's website, www.hepcommjournal.com.

in iHeps (iHeps EMTi), and further characterized their function both in vitro and in vivo analyses.

Results: Inhibition of EMT extended the in vitro culture period of iHeps EMTi from day 24 to day 60. In vitro analysis revealed that, compared to control, iHeps EMTi exhibited significantly higher expression levels of hepatic functional markers and enhanced hepatocyte functions, including lipid accumulation, glycogen storage, albumin secretion, and urea acid metabolism. Moreover, the molecular profiles of iHeps EMTi are closer to those of primary human hepatocytes. In addition, the in vivo engraftment efficiency of iHeps EMTi in the chimeric mice model was also improved as compared to iHeps alone.

Conclusions: We established a robust protocol to generate human iHeps with improved function and capable of long-term in vitro culturing via the suppression of EMT. Moreover, those iHeps with EMT suppression have improved engraftment in human chimeric mice.

Keywords: cell therapy, epithelial–mesenchymal transition, induced pluripotent stem cells, iPSC-induced hepatocytes

INTRODUCTION

The human liver is a pivotal organ that is indispensable for many essential physiological functions. Derived from healthy donors, primary human hepatocytes (PHHs) are widely used in disease modeling, pharmacological testing, and cellular replacement therapies.[1,2] However, PHHs are challenging to maintain and proliferate in vitro or genetic alterations, exhibit significant batch-to-batch variations, and are scarce due to a limited availability of organ donors. As a result, those hurdles limit the applications of PHHs as a platform for research or drug testing, as well as a cell source for therapy. In recent years, human pluripotent stem cells, such as induced pluripotent stem cells (iPSCs), induced hepatocytes (iHeps), have emerged as an unlimited cell source for disease modeling, drug screening, and even autologous cell therapy due to their identical genetic backgrounds to donors.[3,4]

Currently, a variety of protocols have been established to generate iHeps via manipulation of a series of signaling pathways that resemble embryonic liver organogenesis.[4–10,11] On the other hand, the quality of iHeps highly depends on the efficiency and maturity of their differentiation, as they are at best mimicking fetal rather than adult hepatocytes.[10] Moreover, like PHHs, long-term culture of iHeps in vitro is also difficult to maintain, which limits their application for long-term drug screening or modeling of late-onset liver diseases.[4]

Here we describe a robust protocol to generate human iHeps with improved function and capable of long-term in vitro culturing via the suppression of epithelial–mesenchymal transition (EMT). Moreover, those iHeps with EMT suppression have improved engraftment in human chimeric mice.

METHODS

Cell culture

Two human iPSC lines reprogrammed from healthy individuals were used in this study. Because human albumin (hALB) expression marks iHep maturation, most of the experiments in this study utilized a female iPSC line (iPSM0058), where hALB was tagged with the fluorescent reporter protein mCherry using CRISPR/Cas9-mediated homologous recombination (Cell Inspire Bio, product number iPSM0058) (Supplemental Figure S1, Supplemental Digital Content 1, http://links.lww.com/HC9/B969). Another male human iPSC line previously generated in our laboratories (iPS4479) was used to duplicate our in vitro findings on iHeps after EMT suppression.

iHeps differentiation from iPSCs

iHeps were differentiated from human iPSCs using our previously modified 3-step protocol.[12] A cocktail of EMT inhibitors was added into the maturation medium at different time points as described in the Supplemental

Methods, Supplemental Digital Content 1, http://links.lww.com/HC9/B969.

Immunofluorescence staining

iHeps were differentiated on Matrigel-coated coverslips or 4-well chamber slides (Millipore). At certain time points of differentiation, iHeps were fixed with 4% paraformaldehyde. After fixation, cells were washed 3 times with PBS and incubated in blocking buffer (PBS containing 10% donkey serum and 1% Triton X-100 [PBST] for blocking and permeabilization) for 1 hour at room temperature. The primary antibodies were diluted in the blocking buffer at different dilution rates listed in Supplemental Table S1, Supplemental Digital Content 1, http://links.lww.com/HC9/B969. After primary antibody incubation, samples were washed with PBST 3 times before incubation with secondary antibodies at room temperature for 1 hour. Next, the nuclei were stained with DAPI (Sigma-Aldrich, 1: 10000 dilution), and washed with 2 changes of PBST and 2 changes of PBS. Finally, the coverslips or chamber slides were mounted using FlourSave Reagent (Millipore) and observed under a fluorescence microscope (Nikon Eclipse Ni) or confocal microscope (Carl Zeiss, LSM900).

Flow cytometry

The iHeps were dissociated into single cells using Accutase. After dissociation, iHeps were resuspended in PBS containing 1% bovine serum albumin and passed through a 100 μm cell strainer before loading into the machine. As the M0058 iPSC line contains a reporter gene hALB-mCherry, direct flow cytometry was used to detect the percentage of hALB-positive cells, and the undifferentiated iPSC line M0058 was used as a negative control. For iPS4479 iPSC line, the iHeps were incubated with hALB antibody, and then incubated with a secondary phycoerythrin antibody (Alexa Fluor 594) or Donkey anti-Goat IgG before being resuspended in MACS buffer. Similarly, flow cytometry was used to detect the percentage of hALB-positive cells. Results were analyzed using FlowJo.

hALB secretion measurement

We collected 24 hours of supernatant at certain time points for measurement of albumin secretion. Supernatant was diluted from 2× to 20× before measuring with Human Albumin ELISA Quantitation Kit (Bethyl Laboratories) according to the manufacturer's instructions.

Periodic acid-Schiff (PAS) staining

PAS staining was performed using a Periodic acid-Schiff Kit (Sigma-Aldrich) according to the manufacturer's protocol. Cells were fixed using 4% paraformaldehyde for 10 minutes at room temperature before staining.

Oil red O staining

Oil red O stock solution was made by dissolving the oil red O powder (Sigma-Aldrich) into isopropanol to a concentration of 5% (mass/vol). Before staining, the stock solution was diluted with ddH_2O at a ratio of 3:2, then passed through filter paper to make the working solution. iHeps were incubated in freshly prepared working solution for 15 minutes, washed with ddH_2O 3 times, and finally mounted with Faramount Aqueous Mounting Medium (DAKO). Staining results were observed under an optical microscope.

Low-density lipoprotein (LDL) uptake assay

The Dil-LDL (Thermo Fisher Scientific) was diluted in ice-cold HCM to a concentration of 5 μg/mL. iHeps were washed with 3 changes of ice-cold PBS, and the diluted Dil-LDL solution was added to the cells. Next, the whole plate was placed on ice for 5 minutes and then transferred to a 37 °C incubator for 60 minutes. After LDL uptake, iHeps were fixed with 4% paraformaldehyde at room temperature for 10 minutes, mounted with FlourSave Reagent, and observed under a fluorescence microscope.

Urea secretion

Twenty-four hours supernatant was collected from iHeps and urea secretion measured using a Urea Assay Kit (Sigma-Aldrich, MAK006) according to the manufacturer's instructions.

Transplantation of iHeps into FRG mouse livers

All animal experiments were conducted in accordance with the guidelines established by the Committee on the Use of Live Animals in Teaching and Research (CULATR) of the University of Hong Kong.

As described previously,[12,13] 6–8 weeks old immunodeficient Fah-knockout mice ($Fah^{-/-}/Rag2^{-/-}/Il2rg^{-/-}$, FRG mice) were used for iHeps in vivo repopulation. In brief, a total of 0.5 million iHeps per mouse were

transplanted into FRG mouse livers via intrasplenic transplantation.

Alanine aminotransferase

The serum levels of ALT were measured as an indicator of liver cell damage. The ALT activity was determined using a commercially available ALT assay kit following the manufacturer's instructions (Teco Diagnostics ALT [SGPT] Kinetic, A532-150). Serum samples were collected from the FRG mice before sacrifice, and incubated with a substrate solution, and the absorbance was measured at a specific wavelength using a spectrophotometer. The ALT activity was calculated based on the absorbance readings and expressed as units per liter (U/L).

Detailed methods are provided in Supplemental Materials, Supplemental Digital Content 1, http://links.lww.com/HC9/B969.

RESULTS

iHeps undergo EMT during in vitro differentiation

In this study, we employed a 3-stage stepwise protocol to generate iHeps from human iPSCs.[12] This protocol induced iPSCs toward definitive endoderm cells (endoderm induction stage), followed by hepatoblast (hepatic initiation stage), and finally to hepatocytes (hepatocyte maturation stage) (Figure 1A).

Immunofluorescence staining of different cell markers including hALB, carbamoyl-phosphate synthase 1 (CPS1), SRY-box transcription factor 9 (SOX9), alpha-fetoprotein (AFP), and cytokeratin 19 (CK19) on the differentiated cells from day 9 to day 24 to represent mature hepatocytes, hepatic progenitor cells, fetal hepatocytes, and cholangiocytes, respectively, were performed (Supplemental Figures S2A–F, Supplemental Digital Content 1, http://links.lww.com/HC9/B969). The hepatic progenitor marker SOX9 was highly expressed from day 12 to day 18, and then decreased at day 24 (Supplemental Figure S2E, Supplemental Digital Content 1, http://links.lww.com/HC9/B969). On the other hand, the expression of CPS1 and hALB as observed in mature hepatocytes increased from day 15 to day 24 (Supplemental Figures S2A, C, Supplemental Digital Content 1, http://links.lww.com/HC9/B969). These data indicated the fate of hepatocytes in the iHeps differentiation in vitro. Nevertheless, the expression of cholangiocytes marker CK19 and fetal hepatocytes marker AFP was persistently increased and remained high during days 15–24, indicating the immature and biopotential state of iHeps (Supplemental Figures S2E, F, Supplemental Digital Content 1, http://links.lww.com/HC9/B969).

Previous studies have shown that PHHs undergo EMT in vitro, leading to dedifferentiation and eventually loss of hepatic functions, which hinders their further application.[14,15] Interestingly, a similar EMT process occurs at the last stage of iHeps differentiation. During the iHeps maturation stage, we observed an increasing number of spindle-shaped mesenchymal-like cell (Figure 1B, Supplemental Figure 3A, Supplemental Digital Content 1, http://links.lww.com/HC9/B969), and immunostaining showed the expression of alpha smooth muscle actin (α-SMA) in these cells (Figure 1C and Supplemental Figure S2C, Supplemental Digital Content 1, http://links.lww.com/HC9/B969). Quantitative polymerase chain reaction (qPCR) analysis also revealed no changes in the expression of epithelial marker cadherin 1 (CDH1), which were consistent with the immunostaining results (Figure 1D and Supplemental Figure S3B, Supplemental Digital Content 1, http://links.lww.com/HC9/B969). However, the upregulation of EMT markers, including snail family transcriptional repressor 2 (SNAI2), collagen type 1 alpha 1 chain (COL1A1), and actin alpha 2, smooth muscle (ACTA2) were observed in 2 different iPSC lines during the differentiation process (Figure 1D and Supplemental Figure 3B, Supplemental Digital Content 1, http://links.lww.com/HC9/B969). Moreover, we observed a decrease in hALB secretion level and gene expression in iHeps when the duration of in vitro culture extended beyond day 24 of differentiation (Figures 2A, C and Supplemental Figure S3D, Supplemental Digital Content 1, http://links.lww.com/HC9/B969).

Taken together, these findings suggested that the EMT process correlates with decreased cellular function in the later stage of iHeps differentiation.

EMTi enables long-term in vitro culture of iHeps

Prior studies have shown that a combination of small molecules can efficiently inhibit the EMT process of PHHs and maintain their function in vitro for more than 30 days.[16] Accordingly, we hypothesized that using a cocktail of small molecule combinations (SB431542, Forskolin, DAPT, IWP2, and LDN193189, hereafter named as EMTi)[16] can suppress EMT of iHeps and thus maintain their culture for prolonged period in vitro to improve maturation.

Next, we investigated the effects of EMTi on iHeps differentiation and their long-term maintenance in vitro, and monitored their iHeps differentiation efficiency based on the expression of hALB. First, we demonstrated the expression of EMT markers during the differentiation, and qPCR data showed that the EMT process of iHeps started between day 12 and day 15 (Figure 1D and Supplemental Figure 3B, Supplemental Digital Content 1, http://links.lww.com/HC9/B969).

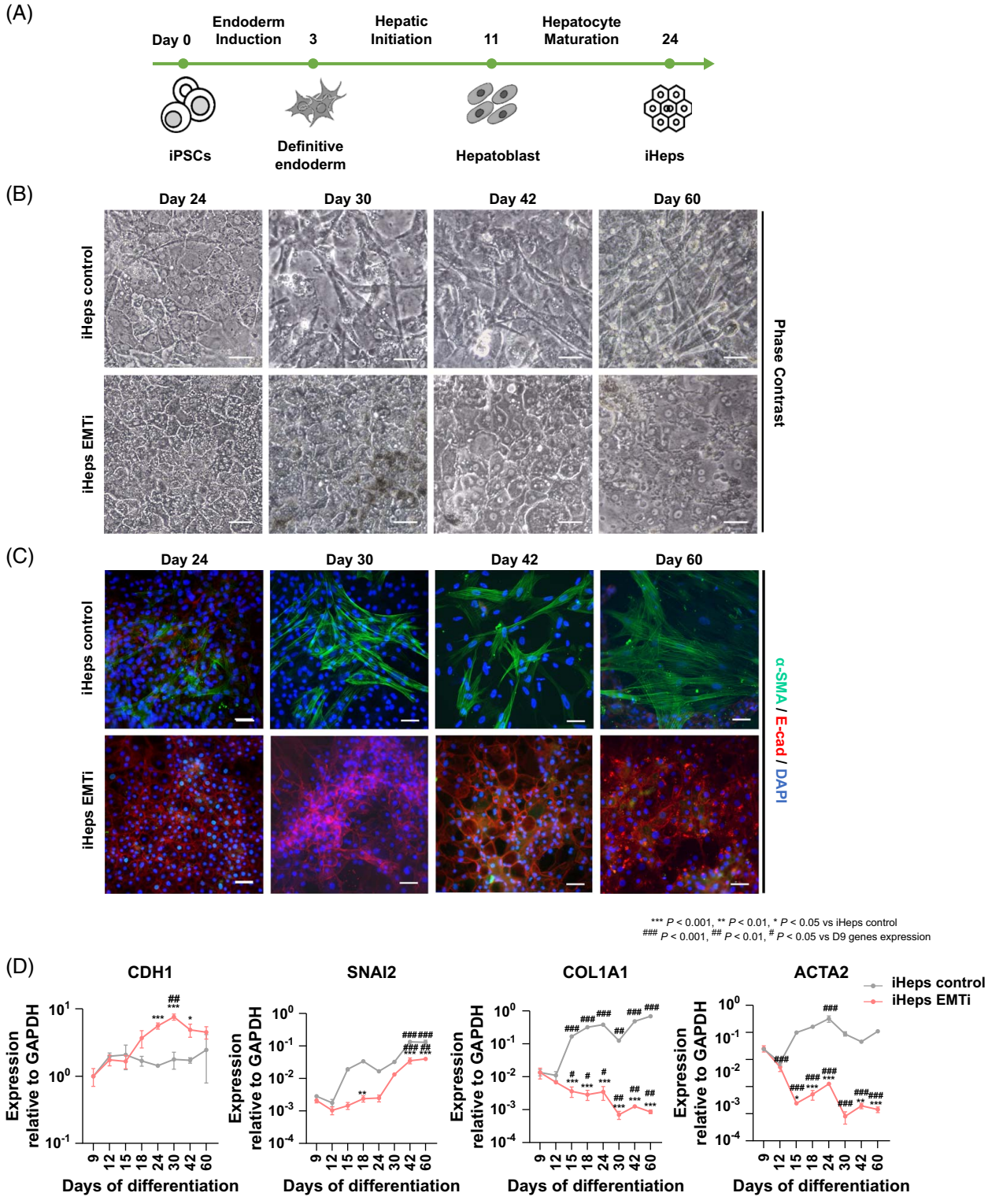

FIGURE 1 iHeps undergo epithelial–mesenchymal transition during long-term in vitro culture. (A) Schematic of iHeps differentiation procedures. (B) Phase contrast images show the morphology of iHeps during 60 days of differentiation. Scale bars represent 50 μm. (C) Immunofluorescence staining for α-SMA and E-cadherin in iHeps control and iHeps EMTi during long-term in vitro culture. Scale bars represent 50 μm. (D) qPCR analysis confirmed the expression of EMT marker genes. For all measurements, n = 3 in both iHeps control and iHeps EMTi groups; $^{*}p < 0.05$, $^{**}p < 0.01$, and $^{***}p < 0.001$ versus iHeps control; $^{\#}p < 0.05$, $^{\#\#}p < 0.01$, and $^{\#\#\#}p < 0.001$ versus D9 gene expression; *p* values were obtained using 2-tailed Student *t* test (*) or one-way ANOVA test (#), error bars indicate SEM. Abbreviations: α-SMA, alpha smooth muscle actin; EMTi, EMT inhibitor; iHeps, iPSC-derived hepatocytes; qPCR, quantitative polymerase chain reaction.

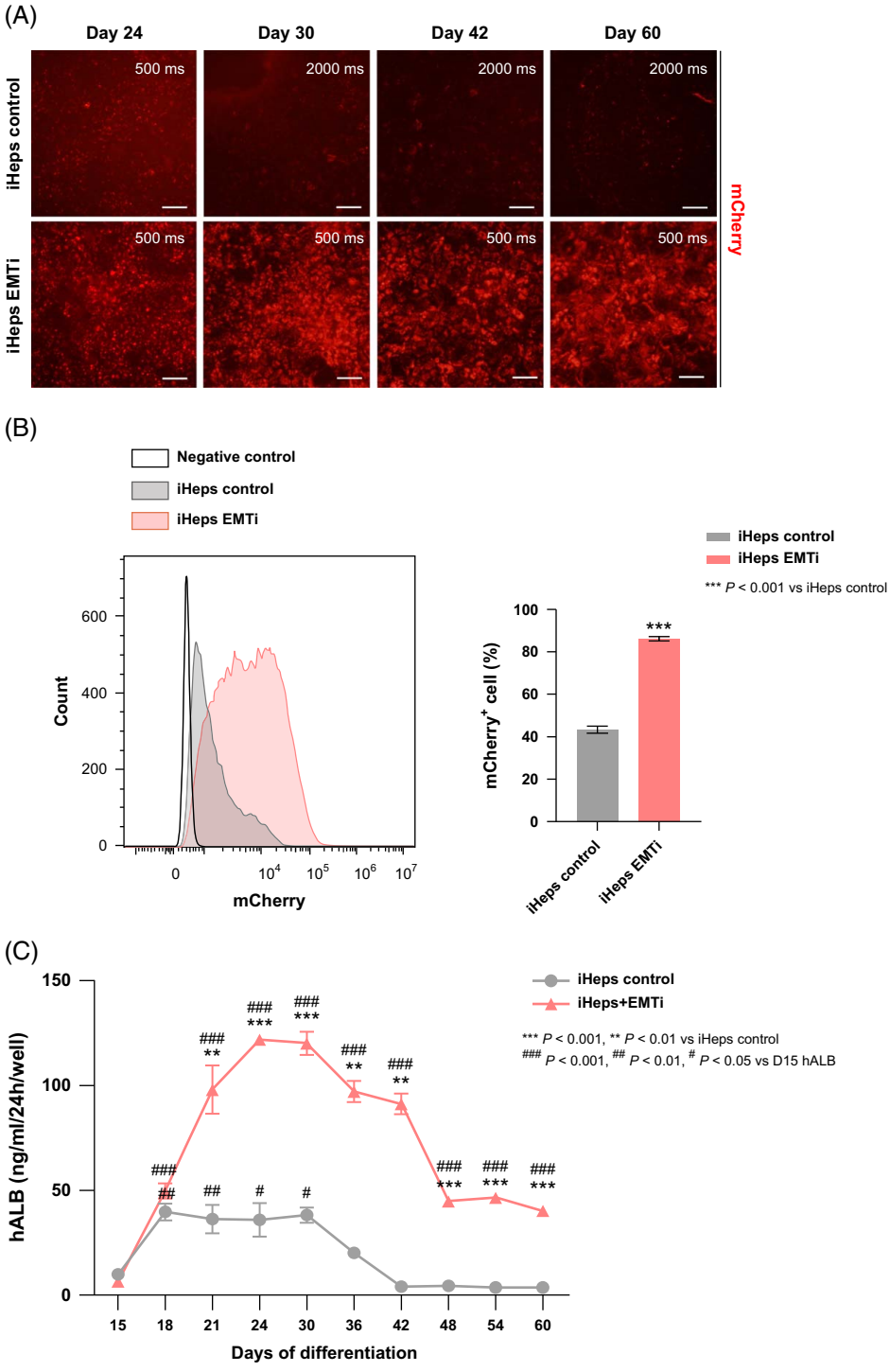

FIGURE 2 Inhibition of EMT benefits iHeps differentiation and long-term in vitro maintenance. (A) Live cell fluorescence images show mCherry expression in each group of iHeps during long-term culture. Exposure time: 2000 ms in the iHeps control group on days 30, 42, and 60; 500 ms in the iHeps EMTi group at day 24 and the iHeps EMTi group at days 24, 30, 42, and 60. Scale bars represent 100 μm. (B) Flow cytometry for mCherry shows the hALB-positive cell rate, indicating iHeps differentiation efficiency. The bar chart shows the quantification of mCherry-positive cell percentage in control and EMTi groups (n = 3). (C) hALB secretion during iHeps long-term culture in vitro. For all measurements, $n \geq 3$ in both iHeps control and iHeps EMTi groups; $^{*}p < 0.05$, $^{**}p < 0.01$, and $^{***}p < 0.001$ versus iHeps control; $^{\#}p < 0.05$, $^{\#\#}p < 0.01$, and $^{\#\#\#}p < 0.001$ versus D15 hALB; *p* values were obtained using 2-tailed Student *t* test (*) or one-way ANOVA test (#); error bars indicate SEM. Abbreviations: EMT, epithelial–mesenchymal transition; EMTi, EMT inhibitor; hALB, human albumin; iHeps, iPSC-derived hepatocytes.

Therefore, we administered EMTi on day 11 of iHeps differentiation before they completed the differentiation by days 18.5–9.16. Furthermore, we maintained the culture up to day 60 to test the effects of EMTi on long-term culturing of iHeps.

As shown in Figure 1B, iHeps differentiated without EMTi (iHeps control) started to form fibroblast-like cells on day 24. In contrast, iHeps with EMTi (iHeps EMTi group) were able to maintain their hepatocyte-like morphologies up to day 60 of in vitro culture. Next, we monitored the EMT-related markers at different time points to confirm the suppression of EMT in the long-term culture of iHeps. By co-staining of the epithelial marker (E-cadherin) and the mesenchymal marker (α-SMA), the iHeps control group showed a large number of α-SMA–positive cells and lost most of the E-cadherin expression cells after day 24 of differentiation (Figure 1C). In contrast, the iHeps EMTi group demonstrated persistent E-cadherin expression without any α-SMA–positive cells up to day 60 of differentiation (Figure 1C). Similarly, qPCR analysis also detected a much higher expression of the epithelial marker CDH1, and significantly lower expression of EMT markers such as SNAI2, COL1A1, and ACTA2 in the iHeps EMTi group as compared to iHeps control group (Figure 1D, Supplemental Figure 3B, Supplemental Digital Content 1, http://links.lww.com/HC9/B969; $p < 0.05$).

Detailed time course co-staining of hepatic markers CPS1 and hALB with EMT transition marker E-cadherin and α-SMA further confirmed the higher expression of E-cadherin and decreased expression of α-SMA from day 24 in the iHeps EMTi group (Supplemental Figure S2A–D, Supplemental Digital Content 1, http://links.lww.com/HC9/B969). Moreover, the expression of CPS1 and hALB and epithelial marker E-cadherin increased during the maturation stage and was maintained at high expression levels up to day 60 in the iHeps EMTi group compared with the iHeps control group (Supplemental Figure S2A–D, Supplemental Digital Content 1, http://links.lww.com/HC9/B969).

Together, these data indicate that suppression of EMT enables the long-term in vitro maintenance of iHeps.

Effects of EMTi on in vitro iHeps differentiation and maturation

EMT occurred on day 11, which is in the maturation stage of iHeps, giving us the opportunity to investigate if the suppression of EMTi could enhance the differentiation and function of iHeps. iHeps EMTi group showed increased expression of hALB after day 24, as shown by the immunostaining of hALB-mCherry reporter as compared to the iHeps control group (Figure 2A). Flow cytometry analysis also demonstrated a significant increase in the percentage of hALB-positive cells, rising from 40% to 80% for the iPSM0052 line and from 60% to 80% for the iPS4479 line in the iHeps EMTi group compared to the iHeps control group (Figure 2B and Supplemental Figure S3C, Supplemental Digital Content 1, http://links.lww.com/HC9/B969; $p < 0.01$). These findings suggest that EMTi can potentially improve iHep differentiation for different iPSC lines.

Moreover, the level of hALB secretion from the iHeps EMTi group was also significantly higher than the iHeps control group at day 18, which was maintained up to day 60 ($p < 0.05$, Figure 2C). Nevertheless, the level of hALB secretion was significantly higher at day 30 as compared to day 60 in the iHeps EMTi group (Figure 2C, $p < 0.05$). Continuous monitoring revealed that the level of hALB secretion peaked around day 30; therefore, liver function assessments and hepatocyte transplantation experiments were conducted using cells differentiated at day 30.

Next, the time course immunostaining of differentiated cells with hepatoblast marker HNF4A, fetal hepatocyte marker AFP, and mature hepatocyte marker hALB indicated that administration of EMTi could enhance the maturation efficiency at different time points (Supplemental Figures S2C, D, F, Supplemental Digital Content 1, http://links.lww.com/HC9/B969). Indeed, qPCR revealed that the increased expressions of different hepatic functional markers, including the transcription factor gene HNF4A, secreted genes hALB, α-1-antitrypsin (AAT) and transferrin (TTR), drug metabolism gene cytochrome P450 3A4 (CYP3A4), detoxification gene UDP glucuronosyltransferase family 1 member A1 (UGT1A1), tyrosine catabolic enzyme fumarylacetoacetate hydrolase (FAH), xenobiotic-responsive gene nuclear receptor subfamily 1 group I member 3 (CAR), urea cycle enzyme CPS1 were significantly higher in the differentiation day 30 iHeps EMTi group than the iHeps control group (all $p < 0.05$; Figure 3A). The increased gene expressions of cytochrome P450 family 7 subfamily A member 1 (CYP7A1), ATP-binding cassette, subfamily B(MDR/TAP), member 11b(BSEP), and CF transmembrane conductance regulator (CFTR) indicated the enhanced bile drainage function of iHeps EMTi, although their expressions level remains lower than that in PHH (Figure 3B).

Further characterization of the in vitro function revealed that the lipid accumulation, glycogen storage (Figure 3C), secretion of urea (Figure 3D), and hALB (Figure 3E) were significantly higher in the differentiation day 30 iHeps EMTi group than the iHeps control group (all $p < 0.05$). The secretion level of albumin from every 1 million iHeps EMTi cells can reach about one-third of that from PHH per day (Figure 3E).

Overall, these data demonstrated that inhibition of EMT could enhance the maturation of iHeps in vitro.

Transcriptional profiling of iHeps with EMTi are closer to PHHs

To further characterize the effects of EMTi on the iHeps differentiation, we performed bulk RNA sequencing on

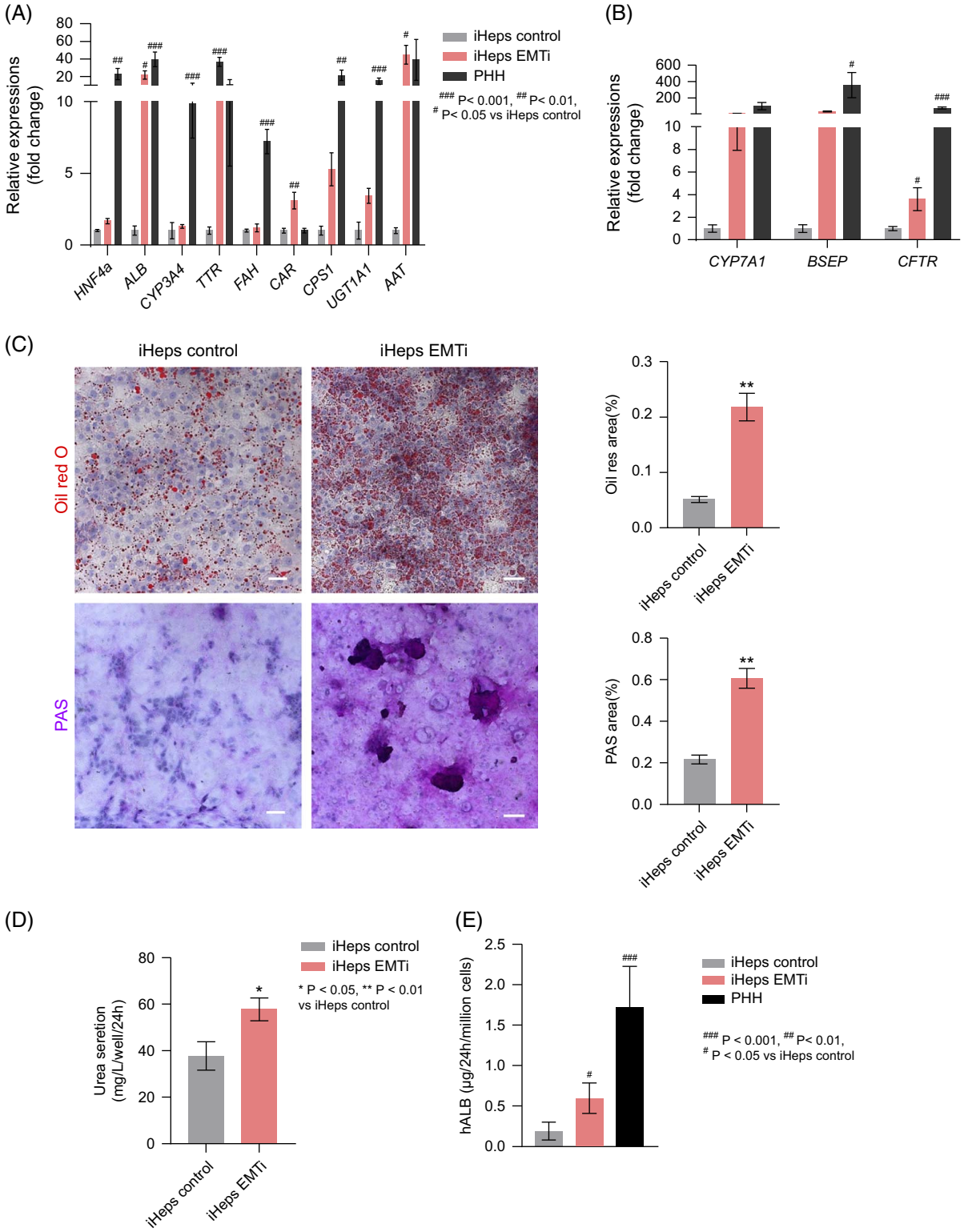

FIGURE 3 Characterization of EMTi optimized iHeps. (A) qPCR analysis shows the expression of hepatic marker genes. For all measurements, n = 6 in both iHeps control and iHeps EMTi groups. (B) Bile drainage gene and mature bile duct gene expressions were measured by qPCR in both iHeps control and iHeps EMTi groups at day 30 of differentiation, with PHH as a positive control. (C) Oil red O and PAS staining show lipid storage and glycogen storage, respectively. The scale bar represents 100 μm. Bar charts are a quantification of percentages of Oil red O and PAS-positive areas. (D) Urea assay shows urea secretion in 2 groups of iHeps. (E) ELISA shows hALB secretion level (μg/mL/24 h/million cells). All scale bars represent 100 μm. For all measurements in this figure, n ≥ 7 in both iHeps control and iHeps+EMTi groups; $^{*}p < 0.05$ and $^{**}p < 0.01$ versus iHeps control; $^{\#}p < 0.05$, $^{\#\#}p < 0.01$, and $^{\#\#\#}p < 0.001$ versus iHeps control; *p* values were obtained using 2-tailed Student *t* test (*) or one-way ANOVA test (#), error bars indicate SEM. Abbreviations: EMTi, EMT inhibitor; hALB, human albumin; iHeps, iPSC-derived hepatocytes; PAS, periodic acid-Schiff; PHH, primary human hepatocyte; qPCR, quantitative polymerase chain reaction.

day 24 iHeps control and iHeps EMTi groups, and 2 different PHH lines were used as positive controls. Principal component analysis revealed a district clustering among different groups of samples (Figure 4A). As expected, the dendrograms showed similar global patterns among the iHeps control, iHeps EMTi, and PHH group (Figure 4B). However, the overall expression of hepatic marker genes was upregulated in the iHeps EMTi group compared to the iHeps control group and was closer to PHHs (Figure 4C). In addition, as compared to the iHeps control, EMT-related genes in the iHeps EMTi group were generally downregulated and similar to the level of PHHs (Figure 4D). Gene set enrichment analysis demonstrated that many metabolic pathways (including amino acid metabolism, xenobiotic metabolism, drug metabolism, etc.) were significantly upregulated in the iHeps EMTi group (Figure 4E).

These transcriptional profile results indicated that the iHeps EMTi group was closer to PHHs than the iHeps control group. Prior studies showed that liver zonation was responsible for liver homeostasis and repair.[17,18] We further analyzed our RNA sequencing data for different zonation markers. Interestingly, the heatmap revealed that zone 1 markers were overall upregulated after iHeps were treated with EMTi (Supplemental Figure S4A, Supplemental Digital Content 1, http://links.lww.com/HC9/B969). Principal component analysis based on different zone marker genes indicated the similarity between iHeps and iHeps EMTi groups, but iHeps EMTi groups were closer to PHHs group than iHeps control groups (Supplemental Figure S4B, Supplemental Digital Content 1, http://links.lww.com/HC9/B969).

Taken together, these findings suggested that EMTi provides sustained and long-term suppression of EMT in iHeps, which subsequently facilitates their long-term culturing and functional maintenance in vitro.

Enhanced in vivo engraftment of iHeps with EMTi

Next, we sought to investigate whether improved in vitro culture and function of iHeps with EMTi can enhance their engraftment in vivo. Fah$^{-/-}$/Rag2$^{-/-}$/Il2rg$^{-/-}$ (FRG) mouse is a hybrid mouse generated by crossing Fah gene knockout mice (which lack tyrosine catabolic enzyme fumarylacetoacetate hydrolase, or FAH) with Rag2$^{-/-}$/Il2rg$^{-/-}$ immunodeficient mice. The FAH deficiency leads to a disorder in tyrosine metabolism, causing the accumulation of fumarylacetoacetate (FAA) and subsequent liver cell damage. To control liver injury during the experimental process, we administered the drug 2-(2-nitro-4-trifluoromethylbenzoyl)-1,3-cyclohexanedione (NTBC) to the mice, which inhibits FAA accumulation. This drug administration enables us to control the degree of liver damage before the transplantation. After NTBC withdrawal, FRG mice will undergo liver failure and die within 30 days unless they receive hepatocyte transplantation. In this study, we transplanted iHeps with or without EMTi into FRG mice via intrasplenic injection,[19–22] and transplantation of PHHs or Matrigel were performed as positive and negative controls, respectively. After 8 weeks, the chimeric mice liver tissues were collected for evaluation of iHeps engraftment (Figure 5A).

Immunohistochemical staining and immunostaining of hALB showed that both iHeps and PHHs, rather than the Matrigel, integrated into the liver parenchyma of FRG mice (Figure 5B and Supplemental Figure S5, Supplemental Digital Content 1, http://links.lww.com/HC9/B969). By calculating the ALB-positive areas, the engraftment efficiency in the iHeps EMTi group was higher compared to the iHeps control group, although both groups were still much lower than the PHHs transplantation group (Figure 5C). Genomic PCR analysis for human Alu fragments further confirmed the integration of iHeps and PHHs inside the mouse livers (Figure 5D). Transplantation of iHeps with or without EMTi or PHHs preserved the body weight of FRG mice after 36 days, as compared to the significant decrease in the Matrigel group due to the progressive decline in their liver function (Figure 5E). Moreover, we did not observe any hepatomegaly or liver size shrinkage after cell transplantation compared to the normal control (no treatment group), or any tumor formation (data not shown). In addition, transplantation of iHeps EMTi and PHHs, but not iHeps, significantly decreased the serum levels of ALT as compared to the Matrigel group (Figure 5F), suggesting that only iHeps EMTi, but not iHeps, provided improvement in liver function of FRG mice, similar to that of PHHs after transplantation.

DISCUSSION

While the utilization of different components of EMTi have been incorporated into some of the protocols for differentiation of iHeps from pluripotent stem cells, the current study confirmed these findings and further demonstrated that the EMT process in the maturation stage hampers iHeps differentiation. Moreover, we demonstrated that inhibition of EMT in the maturation stage of iHeps significantly increased hepatic differentiation efficiency and maintained hepatocytes function in vitro for a prolonged period. To our knowledge, this is the first study to demonstrate that application of EMTi can improve the repopulation of iHeps in vivo and provide therapeutic effects comparable to PHHs transplantation.

Hepatocytes, being epithelial-like cells, closely attach, forming coherent layers with apico-basal polarity.[23] EMT occurs in hepatocytes in a variety of

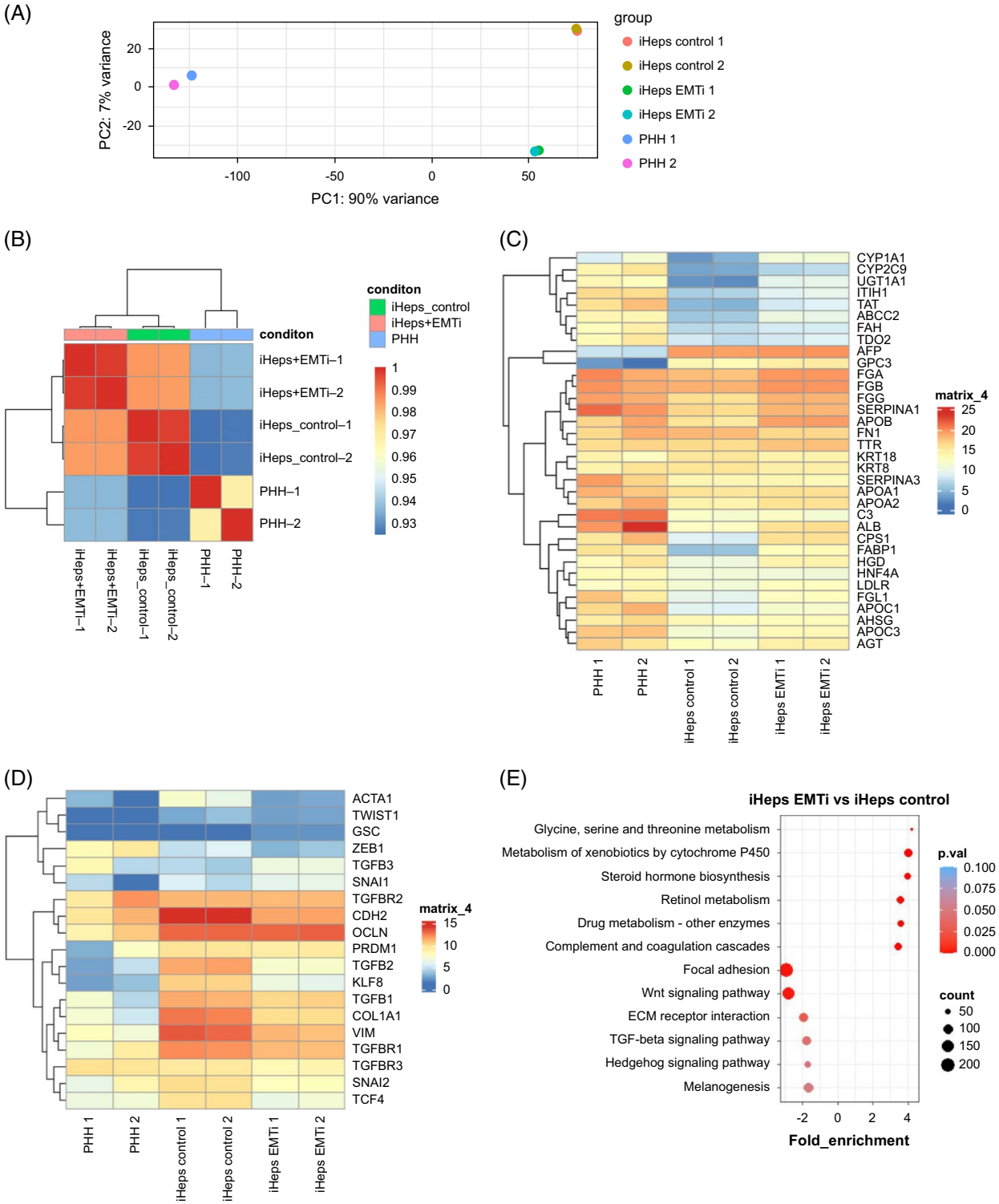

FIGURE 4 RNA-sequencing–based transcriptional profile of iPSC-derived hepatocytes. (A) Principal component analysis (PCA) of PHHs, iHeps control, and iHeps EMTi based on global gene expression profiles. (B) Heatmap of liver gene expression determined by mRNA sequencing comparing 2 independent iHeps, with primary hepatocytes. (C) The heatmap shows the expression of selected hepatic functional genes in different groups of cells. (D) Expression of selected EMT marker genes. (E) Gene set enrichment analysis (GSEA) of differentially expressed pathways between each group of hepatocytes. Abbreviations: EMT, epithelial–mesenchymal transition; EMTi, EMT inhibitor; hALB, human albumin; iHeps, iPSC-derived hepatocytes; iPSC, induced pluripotent stem cell; PAS, periodic acid-Schiff; PHH, primary human hepatocyte; qPCR, quantitative polymerase chain reaction.

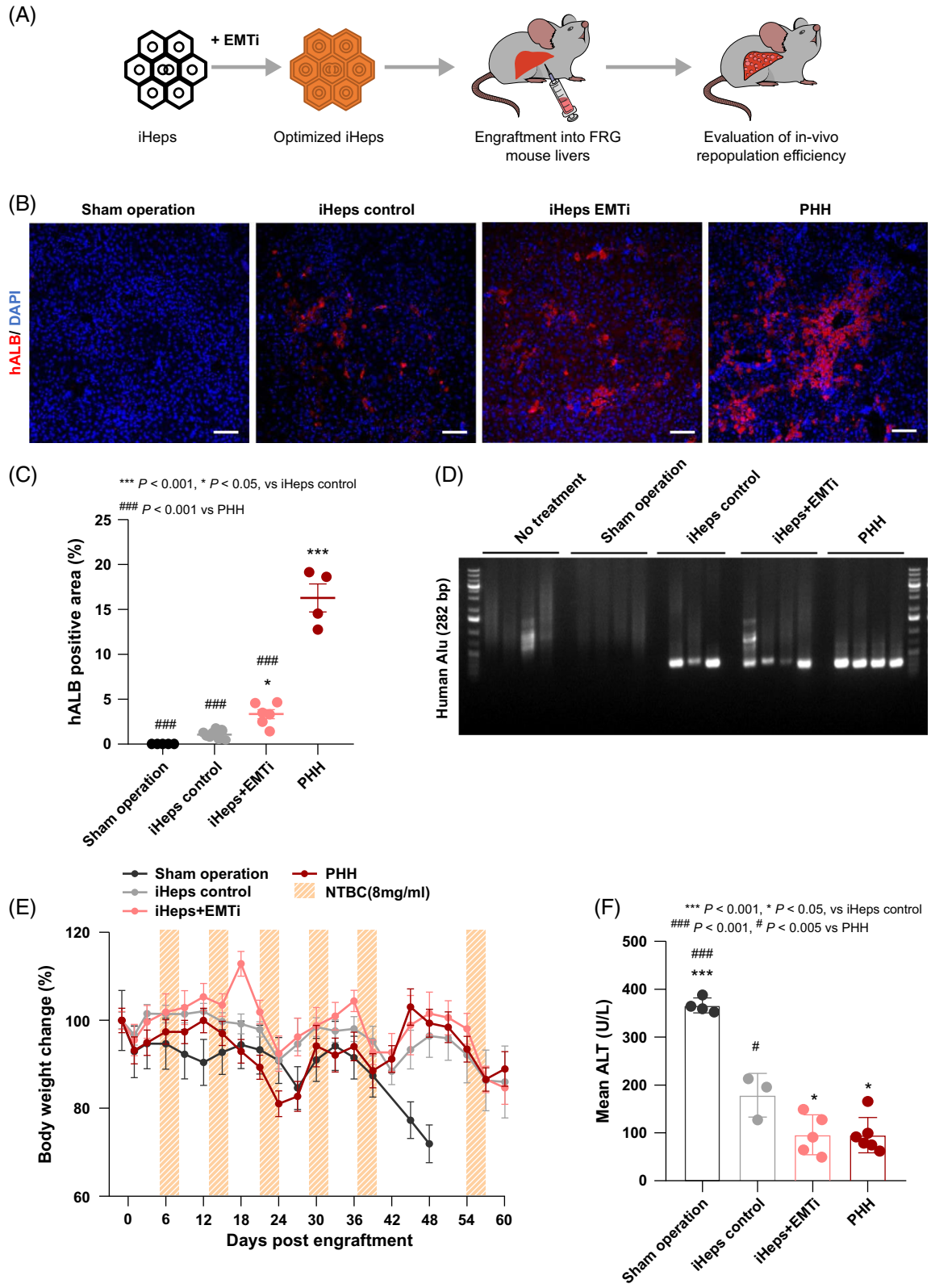

FIGURE 5 Transplantation of iHeps in FRG mouse livers. (A) Schematic of iHeps in vivo repopulation. (B) Representative images of immunofluorescence staining for hALB in mouse liver sections. Scale bars represent 50 μm. (C) Quantification of hALB-positive areas of different groups. n = 5 in sham operation group, n = 8 in iHeps control group, n = 6 in iHeps EMTi group, and n = 4 in PHH group. (D) PCR analysis using primers that specifically recognize the human Alu sequence in genomic DNA isolated from different groups of mouse liver tissue. (E) Body weight change of FRG mice after iHeps transplantation or sham operation. n = 5 in iHeps control group, n = 9 in iHeps EMTi group, n = 9 in PHH group, and n = 5 in sham operation group. Error bars indicate SEM. (F) Plasma ALT level in FRG sham operation mice or FRG mice engrafted with the indicated iHeps or PHH at 4 months post-transplantation (n = 4 in FRG sham operation mice group or FRG mice transplanted with iHeps control

group, n = 5 in FRG mice transplanted with iHeps EMTi, or n = 6 in transplanted with PHH groups; n represents animal number). *$p < 0.05$ and ***$p < 0.001$ versus iHeps control group, #$p < 0.05$ and ###$p < 0.001$ versus PHH group. p values were obtained using one-way ANOVA adjusted with Dunnett multiple comparison; error bars indicate SEM. Abbreviations: EMTi, EMT inhibitor; iHeps, iPSC-derived hepatocytes; hALB, human albumin; PHH, primary human hepatocyte.

different contexts, such as liver organ development,[24] liver regeneration,[25] fibrosis, and neoplasia.[14] The consequences of EMT depend on different biological conditions as well as the cell type in which the process occurs.[14] In our study, we observed an obvious EMT process at the iHeps maturation stage, starting from day 11 of differentiation. The increased expression of myofibroblast markers such as COL1A1 and ACTA2, suggesting that the EMT process during iHeps maturation was more "fibrogenic." Indeed, our results showed that inhibition of EMT either at early (day 11) or late (day 17) time points of the maturation stage led to increased expression of hepatic functional genes and proteins. These findings suggest that the "fibrogenic" EMT induces iHeps toward myofibroblast-like cells, and inhibition of EMT is beneficial to iHeps differentiation and function maintenance in vitro.

Moreover, we observed a substantial increase in iHeps differentiation efficiency after the administration of EMTi. In addition to protecting iHeps from myofibroblast-like cells, it is also possible that EMTi inhibits the differentiation of hepatoblasts toward cholangiocytes, which may further increase the percentage of hepatocytes. From our previous experience,[26] other than hepatocytes, our hepatic differentiation protocol can also give rise to some cholangiocytes. It is known that transforming growth factor beta (TGFβ) and Notch signaling both drive the differentiation of cholangiocytes from hepatoblasts.[22] Since EMTi consists of TGFβ inhibitor and Notch inhibitor, it could also suppress the cholangiocytes differentiation and thus increase the hepatocytes differentiation efficiency. Other than increased differentiation efficiency, iHeps treated with EMTi also exhibited improved in vitro function.

Currently, those pluripotent stem cell-derived iHeps were used between 18 and 25 days of differentiation.[5,8,27,28] Results from previous studies[4] showed that iHeps could hardly be kept functional in vitro for >30 days. Here we demonstrated that the addition of EMTi dramatically elongated the in vitro culture up to at least 60 days to allow more long-term experimental studies as well as potential future use in bioreactors for generating bioartificial livers. Nevertheless, we still observed a progressive decline in the iHeps function in vitro after day 60, as reflected by the reduction in hALB secretion.

It is generally believed that about 10% of liver cells must be replaced to achieve a therapeutic effect in liver cell replacement therapy.[1] However, a very low engraftment rate of iHeps transplantation, as shown in our previous studies and others,[29,30] inevitably hampers their therapeutic application effects. Having optimized the iHeps differentiation in vitro, we also tested the in vivo repopulation capacity by transplanting iHeps with and without EMTi treatment. In this study, the transplantation efficiency of the iHeps control group was around 2%, which was comparable to the results of our previous studies,[4,12] but the engraftment efficiency of EMTi-treated iHeps improved to around 4%. Nevertheless, the engraftment rate of EMTi-treated iHeps was still significantly lower than mature PHH. Previous studies highlighted zone 2 hepatocytes in liver regeneration.[17,18] Indeed, our RNA sequencing data revealed that only the zone 1 markers were overall upregulated, but not the zone 2 markers after treatment with EMTi. This might account for the lack of a significant increase in in vivo repopulation of EMTi-treated iHeps, even though they appear to have higher functional in vitro than those iHeps without EMTi. Moreover, 2D in vitro culture was employed in this study. Recent studies suggest that 3D culture to form liver spheroids/organoids may further enhance the maturation of stem cell-derived induced hepatocytes.[31–34] Furthermore, 3D cultures also inhibited the expression of EMT markers in iPSC-derived liver spheroids.[34] Whether the use of EMTi together with a 3D culture system can further improve the function and engraftment efficiency of iHeps deserves future investigation.

CONCLUSIONS

This study has determined that hiPSC-derived iHeps undergoing "fibrogenic" EMT during the maturation stage are hampered in their maturation and in vitro maintenance. With the addition of EMT inhibitors, we established a robust hepatic differentiation protocol to generate iHeps from hiPSCs with increased maturity and the capability of long-term in vitro maintenance and improved in vivo engraftment.

DATA AVAILABILITY STATEMENT

The data that support the findings of this study are available from the corresponding author (Hung-Fat Tse) upon reasonable request. The RNA-seq data have been deposited in NCBI's Gene Expression Omnibus under the accession number GSE 270003.

AUTHOR CONTRIBUTIONS

Hung-Fat Tse and Rui Wei designed the study. Na Li, Rui Wei, and Yangyang Yuan designed and performed most of the experiments. Mingdan Deng performed all RNA sequencing and analysis. Chi-Wa Cheng assisted in designing and performing the experiments. Jiayin Yang generated the gene-edited iPSC line. Yang Hu

bred the mice and assisted in most of the surgical operations. Wai-In Ho, Ka-Wing Au, Yiu-Lam Tse, Fei Li, Xinyi Wu, Yee-Man Lau, Kwong-Man Ng, Songyan Liao, Stephanie Ma, Pentao Liu, and Miguel A. Esteban supplied experimental materials and resources. Rui Wei, Na Li, Yangyang Yuan, and Hung-Fat Tse analyzed the data and wrote the manuscript.

FUNDING INFORMATION

This work was supported by the Shenzhen-Hong Kong Technology Cooperation Funding Scheme [GHP/130/18/SZ (Hong Kong); SGLH20180627143202102 (Shenzhen)], the Guangdong-Hong Kong Technology Cooperation Funding Scheme [GHP/046/17GD (Hong Kong); 2017B050506007 (Guangdong), and the National Natural Science Foundation of China (81873521).

ACKNOWLEDGMENTS

We thank the Centre for Comparative Medicine Research (CCMR) at the University of Hong Kong for their support with surgical procedures and animal care. We acknowledge the Centre for PanorOmic Sciences (CPOS) at the University of Hong Kong for providing access to imaging and Flow Cytometry equipment. We thank the Centre for Translational Stem Cell Biology for providing a fluorescence microscope for the imaging in the supplemental data. Yangyang Yuan, Mingdan Deng, Songyan Liao, Stephanie Ma, Pentao Liu, Kwong-Man Ng, and Hung-Fat Tse is supported by Health@InnoHK, the Innovation and Technology Commission of the Government of HKSAR.

CONFLICTS OF INTEREST

Jiayin Yang is employed by Cell Inspire Therapeutics. She owns stock in Cell Inspire Biotechnology. Miguel Esteban is employed by BGI Cell Group. The remaining authors have no conflicts to report. Please refer to the accompanying ICMJE disclosure forms for further details.

ETHICS APPROVAL AND CONSENT TO PARTICIPATE

The study adhered to the Declaration of Helsinki. All animal experiments were approved by the Committee on the Use of Live Animals in Teaching and Research (CULATR) of the University of Hong Kong (Project title: Generation of patient-specific humanized mouse model using familial hypercholesterolemia iPSC-derived hepatocytes or hepatic organoids. CULATR Number: 5796-21). The study was reviewed and approved on April 15, 2022.

ORCID

Chi-Wa Cheng https://orcid.org/0000–0001–6164–1512
Jiayin Yang https://orcid.org/0000–0001–9134–1959
Stephanie Ma https://orcid.org/0000–0002–2029–7943
Pentao Liu https://orcid.org/0000–0001–5774–9678
Miguel A. Esteban https://orcid.org/0000–0002–1426–6809
Hung-Fat Tse https://orcid.org/0000–0002–9578–7808

REFERENCES

1. Dhawan A, Puppi J, Hughes RD, Mitry RR. Human hepatocyte transplantation: current experience and future challenges. Nat Rev Gastroenterol Hepatol. 2010;7:288–98.
2. Zeilinger K, Freyer N, Damm G, Seehofer D, Knöspel F. Cell sources for in vitro human liver cell culture models. Exp Biol Med (Maywood). 2016;241:1684–98.
3. Rezvani M, Grimm AA, Willenbring H. Assessing the therapeutic potential of lab-made hepatocytes. Hepatology. 2016;64:287–94.
4. Wei R, Yang J, Cheng C-W, Ho W-I, Li N, Hu Y, et al. CRISPR-targeted genome editing of human induced pluripotent stem cell-derived hepatocytes for the treatment of Wilson's disease. JHEP Rep. 2022;4:100389.
5. Hannan NR, Segeritz CP, Touboul T, Vallier L. Production of hepatocyte-like cells from human pluripotent stem cells. Nat Protoc. 2013;8:430–7.
6. Kajiwara M, Aoi T, Okita K, Takahashi R, Inoue H, Takayama N, et al. Donor-dependent variations in hepatic differentiation from human-induced pluripotent stem cells. Proc Natl Acad Sci U S A. 2012;109:12538–43.
7. Cai J, Zhao Y, Liu Y, Ye F, Song Z, Qin H, et al. Directed differentiation of human embryonic stem cells into functional hepatic cells. Hepatology. 2007;45:1229–39.
8. Si-Tayeb K, Noto FK, Nagaoka M, Li J, Battle MA, Duris C, et al. Highly efficient generation of human hepatocyte-like cells from induced pluripotent stem cells. Hepatology. 2010;51:297–305.
9. Song Z, Cai J, Liu Y, Zhao D, Yong J, Duo S, et al. Efficient generation of hepatocyte-like cells from human induced pluripotent stem cells. Cell Res. 2009;19:1233–42.
10. Baxter M, Withey S, Harrison S, Segeritz CP, Zhang F, Atkinson-Dell R, et al. Phenotypic and functional analyses show stem cell-derived hepatocyte-like cells better mimic fetal rather than adult hepatocytes. J Hepatol. 2015;62:581–9.
11. Sullivan GJ, Hay DC, Park IH, Fletcher J, Hannoun Z, Payne CM, et al. Generation of functional human hepatic endoderm from human induced pluripotent stem cells. Hepatology. 2010;51:329–35.
12. Yang J, Wang Y, Zhou T, Wong LY, Tian XY, Hong X, et al. Generation of human liver chimeric mice with hepatocytes from familial hypercholesterolemia induced pluripotent stem cells. Stem Cell Rep. 2017;8:605–18.
13. Yang J, Wong LY, Tian XY, Wei R, Lai WH, Au KW, et al. A familial hypercholesterolemia human liver chimeric mouse model using induced pluripotent stem cell-derived hepatocytes. J Vis Exp. 2018;139:57556.
14. Choi SS, Diehl AM. Epithelial-to-mesenchymal transitions in the liver. Hepatology. 2009;50:2007–13.
15. Katsuda T, Kawamata M, Inoue A, Yamaguchi T, Abe M, Ochiya T. Long-term maintenance of functional primary human hepatocytes using small molecules. FEBS Lett. 2020;594:114–25.
16. Xiang C, Du Y, Meng G, Soon Yi L, Sun S, Song N, et al. Long-term functional maintenance of primary human hepatocytes in vitro. Science. 2019;364:399–402.
17. Wei Y, Wang YG, Jia Y, Li L, Yoon J, Zhang S, et al. Liver homeostasis is maintained by midlobular zone 2 hepatocytes. Science. 2021;371:371.
18. He L, Pu W, Liu X, Zhang Z, Han M, Li Y, et al. Proliferation tracing reveals regional hepatocyte generation in liver homeostasis and repair. Science. 2021;371:eabc4346.

19. Bissig KD, Le TT, Woods NB, Verma IM. Repopulation of adult and neonatal mice with human hepatocytes: a chimeric animal model. Proc Natl Acad Sci U S A. 2007;104:20507–11.
20. Azuma H, Paulk N, Ranade A, Dorrell C, Al-Dhalimy M, Ellis E, et al. Robust expansion of human hepatocytes in Fah$^{-/-}$/Rag2$^{-/-}$/Il2rg$^{-/-}$ mice. Nat Biotechnol. 2007;25:903–10.
21. Zhang K, Zhang L, Liu W, Ma X, Cen J, Sun Z, et al. In vitro expansion of primary human hepatocytes with efficient liver repopulation capacity. Cell Stem Cell. 2018;23:806–819 e804.
22. Hu H, Gehart H, Artegiani B, LO-I C, Dekkers F, Basak O, et al. Long-term expansion of functional mouse and human hepatocytes as 3D organoids. Cell. 2018;175:1591–1606.e19.
23. Zaret KS, Bort R, Duncan SA. Embryonic development of the liver. In: Arias IM, Alter HJ, Boyer JL, Cohen DE, Shafritz DA, Thorgeirsson SS, Wolkoff AW, eds. The Liver. 6th edn. Wiley-Blackwell; 2020;1:14–22.
24. Li Q, Hutchins AP, Chen Y, Li S, Shan Y, Liao B, et al. A sequential EMT–MET mechanism drives the differentiation of human embryonic stem cells towards hepatocytes. Nat Commun. 2017;8:15166.
25. Oh SH, Swiderska-Syn M, Jewell ML, Premont RT, Diehl AM. Liver regeneration requires Yap1-TGFbeta-dependent epithelial–mesenchymal transition in hepatocytes. J Hepatol. 2018;69:359–67.
26. Wei R. Induced hepatocytes from human induced pluripotent stem cells for liver regeneration (Thesis). The University of Hong Kong (Pokfulam, Hong Kong); 2021.
27. Cayo MA, Cai J, DeLaForest A, Noto FK, Nagaoka M, Clark BS, et al. JD induced pluripotent stem cell-derived hepatocytes faithfully recapitulate the pathophysiology of familial hypercholesterolemia. Hepatology. 2012;56:2163–71.
28. Rashid ST, Corbineau S, Hannan N, Marciniak SJ, Miranda E, Alexander G, et al. Modeling inherited metabolic disorders of the liver using human induced pluripotent stem cells. J Clin Invest. 2010;120:3127–36.
29. Wang Q, Sun D, Liang Z, Wang J, Zhong X, Lyu Y, et al. Generation of human hepatocytes from extended pluripotent stem cells. Cell Res. 2020;30:810–3.
30. Chen Y, Li Y, Wang X, Zhang W, Sauer V, Chang CJ, et al. Amelioration of hyperbilirubinemia in Gunn rats after transplantation of human induced pluripotent stem cell-derived hepatocytes. Stem Cell Rep. 2015;5:22–30.
31. Takebe T, Sekine K, Enomura M, Koike H, Kimura M, Ogaeri T, et al. Vascularized and functional human liver from an iPSC-derived organ bud transplant. Nature. 2013;499:481–4.
32. Broutier L, Andersson-Rolf A, Hindley CJ, Boj SF, Clevers H, Koo BK, et al. Culture and establishment of self-renewing human and mouse adult liver and pancreas 3D organoids and their genetic manipulation. Nat Protoc. 2016;11:1724–43.
33. Takebe T, Sekine K, Kimura M, Yoshizawa E, Ayano S, Koido M, et al. Massive and reproducible production of liver buds entirely from human pluripotent stem cells. Cell Rep. 2017;21:2661–70.
34. Lee G, Kim H, Park JY, Kim G, Han J, Chung S, et al. Generation of uniform liver spheroids from human pluripotent stem cells for imaging-based drug toxicity analysis. Biomaterials. 2021;269:120529.

How to cite this article: Li N, Wei R, Yuan Y, Deng M, Hu Y, Cheng C, et al. Enhancement of hepatic differentiation from induced pluripotent stem cells by suppressing epithelial–mesenchymal transition. Hepatol Commun. 2025;9:e0702. https://doi.org/10.1097/HC9.0000000000000702